Proceedings of the 6th European VLBI Network Symposium
Ros, E., Porcas, R.W., Lobanov, A.P., & Zensus, J.A. (eds.)
June 25th-28th 2002, Bonn, Germany

Models of the brightness temperature distributions in compact, extragalactic radio jets

A. Medici and A. P. Lobanov

Max-Planck-Institut für Radioastronomie, Auf dem Hügel 69, D-53121 Bonn, Germany

Abstract. The brightness temperature distribution is a powerful tool to study the conditions in the extragalactic radio sources and to test the models proposed for the inner jets. In this talk we will present the model which describes the brightness temperature distribution in terms of randomly oriented source and a) a single value for the intrinsic brightness temperature and Lorentz factor or b) a function which describes the distribution of these two parameters.

1. Introduction

The upper limit for the intrinsic brightness temperature (T_0) of the extragalactic radio sources is usually taken around 10^{12} K (Kellermann & Pauliny-Toth 1969), beyond which the inverse Compton effect causes rapid electron energy losses and extinguishes the synchrotron radiation. This idea was revised by Readhead (1994) assuming that the sources are close to the equipartition of the energy between particles and magnetic field. He found that a more reasonable value for the upper limit of the intrinsic brightness temperature is 10^{11} K. Moreover he pointed out that the conditions for the occurrence of the inverse Compton catastrophe are very far from equipartition and suggested that some unknown mechanism maintain the source near the equipartition conditions.

Observed T_0 is modified by the (generally unknown) Doppler factor $\delta_{\rm j}$: $T_{\rm b} \propto T_0 \cdot \delta_{\rm j}^{1/(2-\alpha)}$, where T_0 is the "intrinsic" brightness temperature and α is the optically thin spectral index. This effect requires a statistical approach to be applied, to model the observed distribution $N(T_{\rm b})$ and determine the properties of intrinsic brightness temperature distribution in the AGN.

We have collected from the literature multi-frequency VLBI data for the components (most of which are cores) of more than 600 sources: The Table 1 shows the number of sources in each sample. These samples will be used for modeling the distribution of $T_{\rm b}$ at different frequencies, and probing different spatial scales in the jets using the frequency dependence at the core position (Lobanov 1998; Königl 1981).

The knowledge of the distribution of the intrinsic brightness temperature in the compact radio sources can be used to test the physical models proposed for explaining the nature of the inner jets in active galactic nuclei (AGN). The models proposed (Marscher 1995) can be divided into two categories: in the first, the jet accelerates hydrodynamically from a nozzle and, as the internal energy of the plasma is converted into kinetic energy of bulk flow, the jet Lorentz factor $\Gamma_{\rm j}$ increases along the jet. In the second categories, the central engine produces a highly directed, ultra relativistic $e^- - e^+$ beam that scatters photons produced outside the jet. The scattered photons emit X-Rays and γ-rays, and the recoil decelerates the beam (so that $\Gamma_{\rm j}$ decreases along the jet).

Frequency (GHz)	N	References
1.6	90	CJ1, Polatidis et al. (1995), Thakkar et al. (1995)
5	82	CJ1, Xu et al. (1995)
5	190	CJ2, Taylor et al. (1994), Henstock et al. (1995)
5	349	VLBApls, Fomalont et al. (2000)
22	137	Moellenbrock et al. (1996)
43	35	Lister & Marscher (1997)
86	100	Lobanov et al. (2000, 2002)

Table 1. Number of sources in each sample

The distribution of T_0 and $\Gamma_{\rm j}$ can also be used to discriminate between the models proposed for the generation of radiating particles which occur very close to the VLBI core (Marscher 1995). In one of these models the relativistic $e^- - e^+$ pairs are produced through the interactions of the ambient photon field and subsequent particle cascade; in the other one an ultra relativistic neutron beam is emitted by the central engine and then the neutrons decay into protons and electrons which form a relativistically flowing plasma after interacting with the ambient medium. The intensity profiles along the jet (and the resulting brightness temperatures) are significantly different, and have a characteristic shape, in each of these models. This difference can be used to test the models by applying the dependence of T_0 on the observing frequency determined from a statistical modeling

In this paper we develop statistical models to model the distribution of $T_{\rm b}$. In Sect. 2, we discuss the model proposed by Lobanov et al. (2000) and expand it to better describe the observed population of the radio sources. In Sect. 3, we describe the program developed for this purpose and, in Sect. 4, we show some preliminary results

applying this model to synthetic samples and to one of the samples collected from the literature.

2. Population models for the brightness temperature in the jets

In the simplest case (Lobanov et al. 2000) the observed distribution of T_b can be described using the following assumptions:

- jets have the same Lorentz factor Γ_j;
- jets have the same spectral index α, ($S \propto \nu^\alpha$);
- jets have the same intrinsic brightness temperature T_0;
- jets are randomly oriented along the line of sight and are straight within the spatial scale probed by the observation.

These hypotheses yeld the following brightness temperature distribution:

$$P(T_1, T_2) = 2\pi\eta_T \int_{\vartheta(T_1)}^{\vartheta(T_2)} \sin\vartheta \,\mathrm{d}\vartheta, \tag{1}$$

where ϑ is the viewing angle and η_T is the normalisation factor.

This models has the merit of being analytically computable, but the single value assumptions made for T_0 and γ put some limitations to it. To relax these assumptions we have developed a set of more complex models that take into account the distribution law for T_0 and Γ_j. We have considered two different distribution laws for each parameter: 1) Gaussian ($f_\mathrm{g}(x) = \frac{1}{\sqrt{2\pi}\,\sigma_x}\,\mathrm{e}^{-(x-m_x)^2/(2\sigma_x^2)}$) and 2) power law ($f_\mathrm{p}(x) = b\cdot x^a$). Depending whether the previous equations describe $N(T_0)$ or $N(\Gamma_\mathrm{j})$, x, m_x and σ_x are T_0 or Γ_j and their mean and rms; a and b are the exponent and the constant of the power law.

we have then combined the two distribution laws and the single value distribution obtaining 9 different models.

2.1. Gaussian distributions of $N(T_0)$ and $N(\Gamma_\mathrm{j})$

Using the Gaussian distribution for both T_0 and γ, the probability $P(T_1 \le T_\mathrm{b} \le T_2)$ is given by:

$$P(T_1, T_2) =$$

$$= \frac{1}{2\pi\sigma_x\sigma_y} \int_{\vartheta_1}^{\vartheta_2}\int_{T_1}^{T_2}\int_{\Gamma_1}^{\Gamma_2} e^{-\frac{(T-m_T)^2-(\Gamma-m_\Gamma)^2}{(4\sigma_T\sigma_\Gamma)}} \sin\vartheta \,\mathrm{d}\Gamma \,\mathrm{d}T \,\mathrm{d}\vartheta. \tag{2}$$

2.2. Power law distributions of $N(T_0)$ and $N(\Gamma_\mathrm{j})$

If T_0 and γ are both distributed as a power law, we obtain:

$$P(T_1, T_2) =$$

$$= b_T b_\Gamma \int_{\vartheta_1}^{\vartheta_2}\int_{T_1}^{T_2}\int_{\Gamma_1}^{\Gamma_2} T^{a_T}\Gamma^{a_\Gamma} \sin\vartheta \,\mathrm{d}T \,\mathrm{d}\Gamma \,\mathrm{d}\vartheta. \tag{3}$$

2.3. Gaussian and power law

Describing Γ_j with a power law and T_0 with a Gaussian distribution we obtain:

$$P(T_1, T_2) =$$

$$= \frac{b_\Gamma}{\sqrt{2\pi}\sigma_T^2} \int_{\vartheta_1}^{\vartheta_2}\int_{T_1}^{T_2}\int_{\Gamma_1}^{\Gamma_2} \mathrm{e}^{-\frac{(T-m_T)^2}{(2\sigma_T^2)}} \Gamma^{a_\Gamma} \sin\vartheta \,\mathrm{d}T \,\mathrm{d}\Gamma \,\mathrm{d}\vartheta. \tag{4}$$

To obtain the equation for γ described by a Gaussian distribution and T_0 by a power law it is sufficient to swap Γ_j for T_0.

2.4. Gaussian distribution and single value

Combining a Gaussian distribution for T_0, and the single value for Γ_j, we have:

$$P(T_1, T_2) =$$

$$= \frac{1}{\sqrt{2\pi}\sigma_T^2} \int_{\vartheta_1}^{\vartheta_2}\int_{T_1}^{T_2} \mathrm{e}^{-\frac{(T-m_T)^2}{(2\sigma_T^2)}} \sin\vartheta \,\mathrm{d}T \,\mathrm{d}\vartheta. \tag{5}$$

The equation for Γ_j described by a Gaussian distribution and T_0 described by the single value, is:

$$P(T_1, T_2) =$$

$$= \frac{1}{\sqrt{2\pi}\sigma_\Gamma^2} \int_{\vartheta_1}^{\vartheta_2}\int_{\Gamma_1}^{\Gamma_2} \mathrm{e}^{-\frac{(\Gamma-m_\Gamma)^2}{(2\sigma_\Gamma^2)}} \sin\vartheta \,\mathrm{d}\Gamma \,\mathrm{d}\vartheta. \tag{6}$$

2.5. Power law distribution and single value

Finally, describing T_0 with a power law distribution and Γ_j with a single value give:

$$P(T_1, T_2) =$$

$$= b_T \int_{\vartheta_1}^{\vartheta_2}\int_{T_1}^{T_2} T^{a_T} \sin\vartheta \,\mathrm{d}T \,\mathrm{d}\vartheta. \tag{7}$$

For the opposite case:

$$P(T_1, T_2) =$$

$$= b_\Gamma \int_{\vartheta_1}^{\vartheta_2}\int_{\Gamma_1}^{\Gamma_2} \Gamma^{a_\Gamma} \sin\vartheta \,\mathrm{d}\Gamma \,\mathrm{d}\vartheta. \tag{8}$$

3. The calculation of the models

The models described in the previous section are not, in general, fully analytically tractable. Therefore, we have applied the Monte Carlo simulation to calculate the model for all scenarios.

T_0 and Γ_j are calculated from their distribution laws, together with the random angle along the line of sight. Then, using the equation

$$T_b = T_0 \left(\Gamma_\mathrm{j}\,(1 - \sqrt{1-\Gamma_\mathrm{j}^{-2}}\,)\cos\vartheta\right)^{-1/\varepsilon} \tag{9}$$

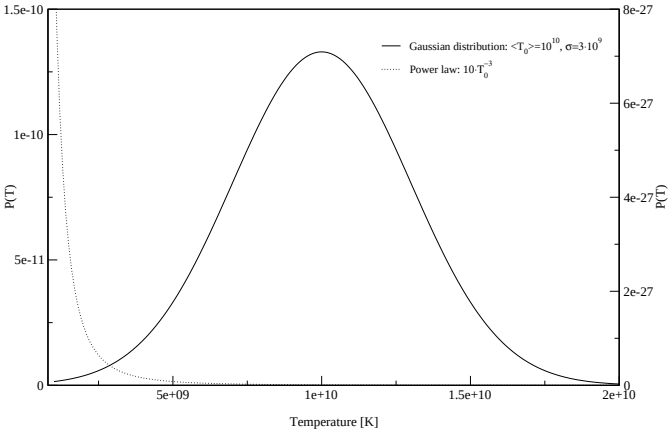

Fig. 1. Examples of the T_0 distributions used in the models.

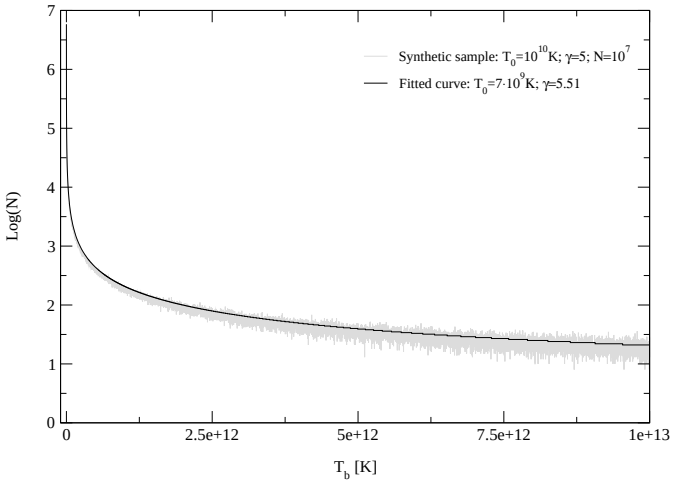

Fig. 2. Distribution of T_b in a sample of 10^{10} sources.

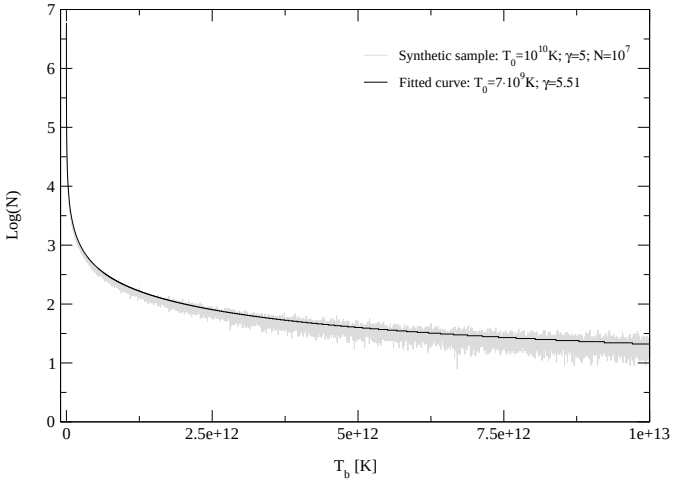

Fig. 3. Distribution of T_b in a sample of 10^{10} sources. For 25% of the sources T_b is a lower limit.

the observed brightness temperature in the rest frame of the source is computed.

To avoid long calculation times, we have used the "gradient method" for finding the minimum value of the χ^2 between the observed and the calculated distributions. The "gradient method" starts by dividing the n-dimensional space (where n can be 3 or 4) of the parameters into a number of equal-area cells and calculating the sum of the χ^2 at the 2^n vertices. Once the cell with the minimum χ^2 has been found, we start to calculate the gradient between the centre of the cell itself and other $n \cdot 2^{n-1}$ points placed in the vertices and in the middle of the edges of a new cell smaller than the original one. The point which gives the steeper negative gradient became the centre of a new cell and the new gradients are calculated until all of the gradients are positive.

4. The simulation

To check the method, we apply the program to a few synthetic samples of radio sources. We create a sample of 10^7 sources with the same $T_0 = 10^{10}$ K and $\Gamma_\mathrm{j} = 5$, flux density randomly distributed between 10^{-3} and 10 Jy, and the viewing angle randomly distributed between 0 and 2π. Since, in real observations, for several objects we have only upper limits for their size and, consequently, only lower limits for T_b, we have simulated this effect creating five samples in which 0%, 25%, 50%, 75% and 90% of the sources have a lower limit for T_b.

We apply then our program specifying that T_0 and Γ_j must be described by a single value. Figures 2–6 show the results of the modeling. In all cases the values found by the program are not too far from the synthetic ones; the error on Γ_j is 10% for all but one sample, and the modelled T_0 is within 20–30% from the synthetic value. The presence of a high number of lower limits does not seem to affect significantly the computation of the values.

As an example we apply the program to the VLBApls sample at 5 GHz (Fomalont et al. 2000). The result is shown in Fig. 7.

5. Conclusions

In this paper we have discussed a set of statistical models that can be applied for modelling the brightness temperature distribution observed in radio sources. We take into consideration the possibilities for T_0 and Γ_j to be represented by a single value, a Gaussian distribution or a power law. The program we have developed can calculate the values of T_0 and Γ_j with a satisfactory precision.

References

Fomalont, E. B., Frey, S., Paragi, Z., et al. 2000, ApJS, 131, 95
Henstock, D. R., Browne, I. W. A., Wilkinson, P. N., et al. 1995, ApJS, 100, 1
Kellermann, K. I. & Pauliny-Toth, I. I. K. 1969, ApJ, 155, L71
Königl, A. 1981, ApJ, 243, 700
Lister, M. L. & Marscher, A. P. 1997, ApJ, 476, 572
Lobanov, A. P. 1998, A&A, 330, 79

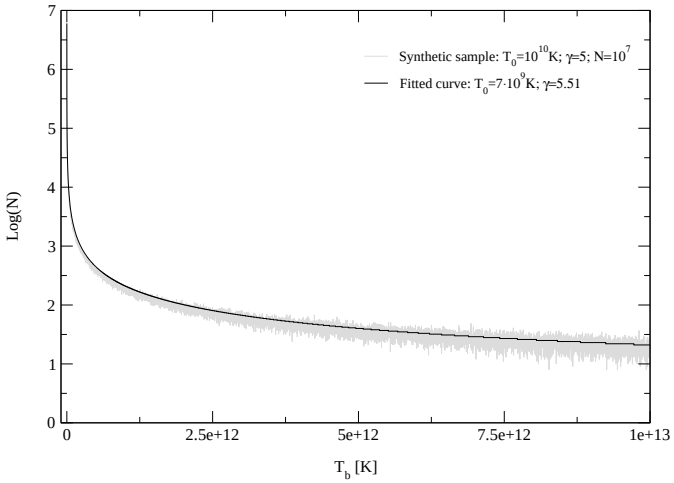

Fig. 4. Distribution of $T_{\rm b}$ in a sample of 10^{10} sources. For 50% of the sources $T_{\rm b}$ is a lower limit.

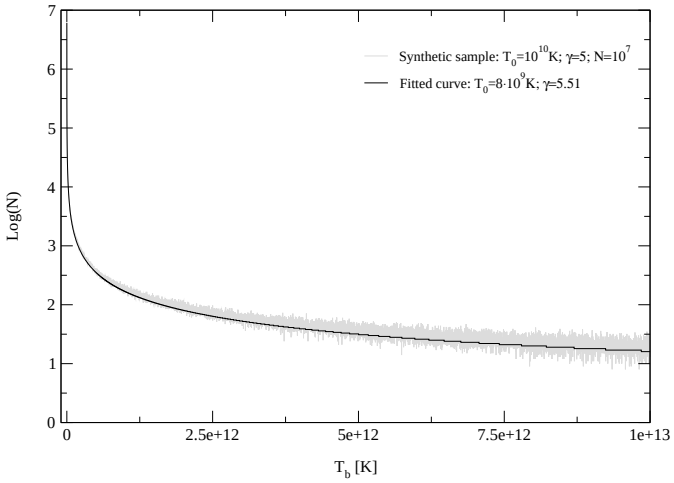

Fig. 5. Distribution of $T_{\rm b}$ in a sample of 10^{10} sources. For 75% of the sources $T_{\rm b}$ is a lower limit.

Lobanov, A. P., Krichbaum, T. P., Graham, D. A., et al. 2002, these proceedings
Lobanov, A. P., Krichbaum, T. P., Graham, D. A., et al. 2000, A&A, 364, 391
Marscher, A. P. 1995, PNAS, 92, 11439
Moellenbrock, G. A., Fujisawa, K., Preston, R. A., et al. 1996, AJ, 111, 2174
Polatidis, A. G., Wilkinson, P. N., Xu, W., et al. 1995, ApJS, 98, 1
Readhead, A. C. S. 1994, ApJ, 426, 51
Taylor, G. B., Vermeulen, R. C., Pearson, T. J., et al. 1994, ApJS, 95, 345
Thakkar, D. D., Xu, W., Readhead, A. C. S., et al. 1995, ApJS, 98, 33
Xu, W., Readhead, A. C. S., Pearson, T. J., Polatidis, A. G., & Wilkinson, P. N. 1995, ApJS, 99, 297

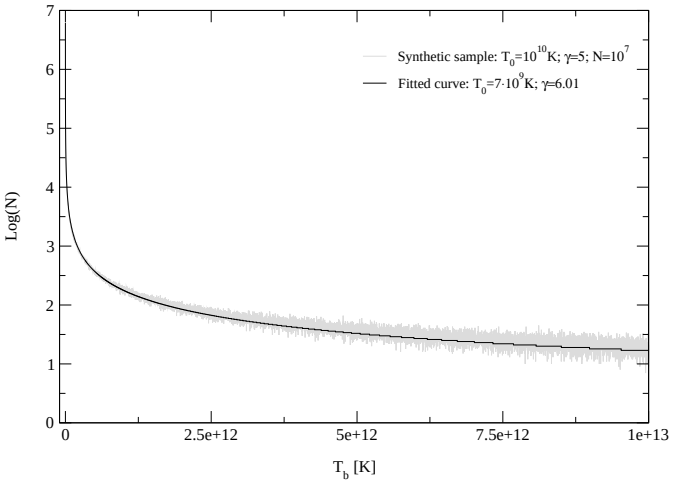

Fig. 6. Distribution of $T_{\rm b}$ in a sample of 10^{10} sources. For 90% of the sources $T_{\rm b}$ is a lower limit.

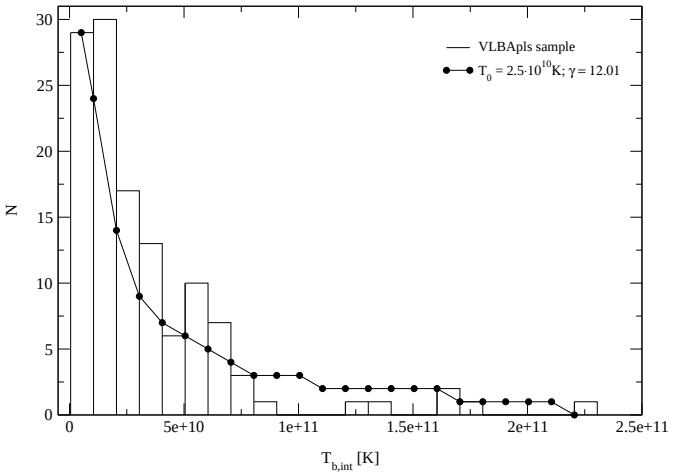

Fig. 7. distribution of the measured brightness temperatures at 5 GHz. The bin size is 10^{10} K. The solid line represents the modelled distribution.